International Journal of Technology (2018) 6: 1225-1235
ISSN 2086-9614

SYNTHESIS OF LTO NANORODS WITH AC/NANO-Si COMPOSITE AS ANODE MATERIAL FOR LITHIUM-ION BATTERIES

Anne Zulfia[1*], Yohana Ruth Margaretha[1], Bambang Priyono[1], Achmad Subhan[2]

[1]*Department of Metallurgical and Materials Engineering, Faculty of Engineering, Universitas Indonesia, Kampus UI Depok, Depok 16424, Indonesia*
[2]*Center of Research for Physics, Indonesian Institute of Science (LIPI), PUSPIPTEK 15314, South Tangerang, Indonesia*

(Received: March 2018 / Revised: July 2018 / Accepted: October 2018)

ABSTRACT

In this study, the synthesis of lithium titanate (LTO) composite with 3 wt% activated carbons (AC) and 10 wt%, 15 wt%, as well as 20 wt% of nano silicon (nano-Si) are carried out. LTO has zero-strain characteristics and has a long life cycle. However, its capacity is limited, and it has poor electrical conductivity. The addition of nano-Si aims to enhance its capacity, while the AC aims to provide a large specific surface area to increase electrical conductivity. The nanorod templates are made from titanium dioxide (TiO_2), which is obtained from titanium (IV) butoxide using the sol–gel method. Nanorod structures are achieved by a hydrothermal process in a 10 M sodium hydroxide (NaOH) solution. However, needle-like structures are also observed, and the Li_2TiO_3 phase is finally formed. Battery performance is determined by CV, CD, and EIS tests. EIS results show that the highest electrical conductivity is found in LTO only; the CV test results show that the highest specific capacity is found in LTO–AC/15% nano-Si, at 140.7 mAh/g, as well as a charge–discharge (CD) capacity at a current rate of 0.2 to 20 C.

Keywords: Activated carbon; Li_2TiO_3; Lithium-ion battery; Lithium titanate; Nano silicon

1. INTRODUCTION

The lithium-ion battery is a promising electric energy resource. It has several advantages over other energy storage methods, including its high cell voltage, the fact that it does not contain a dangerous substance, and its high volumetric and gravimetric density (Cai et al., 2010). The lithium-ion battery has a theoretical energy density of ~400 $Whkg^{-1}$, higher than that of a conventional lead–acid battery, which has an energy density of 30–40 $Whkg^{-1}$, or nickel–cadmium (Ni-Cd) battery, which has an energy density of 40–60 $Whkg^{-1}$ (Girishkumar et al., 2010). This means a lithium-ion battery could be used as an energy resource for electric vehicles, enabling a driving distance of ~400 km per charge (Yoon et al., 2010).

Graphite is the material that is commonly used as an anode for a lithium-ion battery. However, a lithium dendrite structure is formed on the surface of the graphite anode because of short circuits after long-term charge–discharge (CD), especially when the battery is operated under 0.2 V vs. Li/Li^+ (Kuo & Lin, 2014). In the first cycle of CD, a passivating solid electrolyte interface (SEI) layer is formed on the graphite surface because of the low Li^+ insertion potential (<1 V vs. Li^+/Li) (Aurbach et al., 2002). This SEI layer causes bad battery performance.

* Corresponding author's email: anne@metal.ui.ac.id, Tel. +62-81-29017857, Fax. +62-21-8616626
Permalink/DOI: https://doi.org/10.14716/ijtech.v9i6.2444

Therefore, lithium titanate (LTO) is used as the graphite substitute. LTO has a zero-strain characteristic because, during the intercalation and de-intercalation process, the changes of volume that happen are only ~0.2%. This is because the Li^+ ion size is the same as the place in the crystal structure, meaning there is almost no expansion or diminution when an ion enters or leaves the crystal structure (Lu et al., 2007). Nevertheless, LTO has a low theoretical capacity (175 mAh/g) and a low conductivity (10^{-8} – 10^{-13} S/cm) (Zhao et al., 2015). These problems can be solved by reducing the size of the LTO particles and combining them with other materials.

The reduction of LTO particles into nano-size particles will increase the contact area between electrode and electrolyte and shorten the diffusion path between the two. This means the LTO rate capability will increase (Bresser et al., 2012). Previous research found that nanorods' structure provides more electrons channel, has a high surface-to-volume ratio, and has a short diffusion path that will increase the electrochemical performance (Li et al., 2009; Zhou et al., 2015).

Activated carbon (AC) is added to LTO to increase its conductivity and thermal stability. With its addition, the surface area and lithium diffusion increase, resulting in good electrical conductivity (Wang et al., 2007). Silicon has an excellent theoretical capacity of 4,200 mAh/g (Zhou et al., 2014). However, volume changes of ~300% occur during the lithiation and delithiation process, because the silicon cracks during cycling, resulting in irreversible capacity loss (Beaulieu at al., 2001; Maranchi et al., 2003; Zhang et al., 2012). Silicon also has low conductivity (6.7×10^{-4} S cm^{-1}) (Chen et al., 2011; Li et al., 2012;), and an oxide layer forms on the surface (Li et al., 2007; Gao et al., 2011). This problem can be solved by reducing the particle size and combining the silicon with a conductive element such as carbon (Stankulov et al., 2009). This experiment will conduct the synthesis of LTO nanorods with the addition of AC and nano silicon (nano-SI) to increase the electrochemical performance of LTO.

2. METHODS

2.1. Materials Synthesis

2.1.1. Synthesis of LTO

Titanium dioxide (TiO_2) was obtained from titanium (IV) butoxide reagent grade 97% (Sigma Aldrich) using the sol–gel method (Syahrial et al., 2016). The first precursor was a primary solution that consisted of 40 ml ethanol (pH 3) and 6.80 gr of titanium (IV) butoxide. The secondary solution consisted of 10 ml ethanol (pH 3) and 1.26 gr of Aqua Des. The secondary solution was added to the primary solution, while being stirred by a magnetic stirrer. The mixed solution was stirred for 45 minutes until it became solid (gel). The TiO_2 xerogel was calcined for 45 minutes at a rate of 4°C min^{-1} at 300°C (Priyono et al., 2015). After that, 1 gr of TiO_2 was added to a 4 M sodium hydroxide (NaOH) solution, and both were mixed for 30 minutes using a magnetic stirrer. The mixed solution then was transferred to an autoclave and heated at 180°C for 24 hours. The solution was acid washed, using a 0.1 M hydrogen chloride (HCl) solution, until neutral. The outcome was separated using membrane filters and dried in a hot plate at 80°C for 45 minutes. The TiO_2 powder and lithium hydroxide (LiOH) powder were mixed in a ball mill for 30 minutes to form $Li_4Ti_5O_{12}$. The stoichiometric amount was 4.3934 gr TiO_2 mixed with 1.0533 gr LiOH powder. The mixture was sintered at the rate 5°C min^{-1} until it reached the final temperature at 750°C for 1 hour. The result of this process was LTO powder.

2.1.2. Activated carbon

The carbon activation process began with heating the carbon powder at 500°C for 2 hours at a rate 20°C min^{-1}. Based on previous research, carbon was mixed with NaOH at a ratio of 1:3 (wt%) (Cazetta et al., 2011). An NaOH pellet was first diluted in 10 ml Aqua Des. Then, the mixture of carbon and NaOH solution was stirred for 2 hours using a magnetic stirrer and then heated at

130°C for 4 hours. The slurry was then sintered at 700°C for 1.5 hours, at a rate 20°C min^{-1}, under N_2 flow. The dry mixture was washed with 0.1 M HCl solution and hot distilled water and was then separated using membrane filters. The outcome was dried at 110°C for 24 hours, resulting in AC powder.

2.1.3. Synthesis of LTO–AC/nano-Si composite

The LTO and AC were first mixed to form LTO–AC by grinding them on an agate mortar. The amount of AC used was 3 wt%, so the amount of LTO was 97 wt%. Nano-Si powder was obtained from Shanghai yunfu Nanotechnology. The LTO–AC and nano-Si powder were then mixed by grinding the materials on an agate mortar, using the compositions presented in Table 1. The results were LTO–AC/10% nano-Si, LTO–AC/15% nano-Si, and LTO–AC/20% nano-Si.

The coin cells were assembled and used for electrochemical measurements. A binder and conductive agent were added to make a slurry. This research used polyvinylidene fluoride (PVDF) as the binder and acetylene black as the conductive agent. The ratio between active materials, binder, and conductive agent was 8:1:1. All the materials were added to 6 gr of Dimethylacetamide (DMAc), which had already been stirred using a magnetic stirrer. The mixture was stirred for 3 hours while heated at 80°C. The slurry was coated in copper (Cu) foil using a doctor blade and dried at 80°C for 1 hour. The battery was assembled inside a glove box under a vacuum atmosphere.

Table 1 Mass composition of each sample

Material	Mass (gram)	
	Nano-Si	LTO–AC
LTO-AC/10% nano-Si	0.2	1.8
LTO-AC/15% nano- Si	0.3	1.7
LTO-AC/20% nano- Si	0.4	1.6

2.2. Material Characterization

The samples were characterized through scanning electron microscopy (SEM) and energy dispersive X-ray spectroscopy (EDX), using a VEGA 3 TESCAN to determine the morphology, identify the content, and determine the distribution of the content of each composite. An X-ray powder diffraction (XRD) test was used to identify the phase and content of each composite. The surface area of each element was determined by Brunauer–Emmett–Teller (BET) theory using Quantachrome Instruments, with N_2 at 77.350 K.

2.3. Electrochemical Measurement

Battery performance was tested using cyclic voltammetry (CV), CD, and electrochemical impedance spectroscopy (EIS). The CV test was done to determine the insertion and extraction voltage and specific capacity. The performance of the battery and the CD capacity were determined by CD test. The EIS test was done to identify the resistance and conductivity of the materials.

3. RESULTS AND DISCUSSION

3.1. Analysis of LTO Composite by SEM–EDX

The hydrothermal process is supposed to form nanorods of TiO_2 in order to achieve LTO in the nanorod structures. Unfortunately, after the synthesis process, the LTO showed needle-like structures, as shown in Figure 1a. The average width of the needle-like structures was 160 nm, and the average length was 1.8 μm. The image (Figure 1a) also shows agglomeration in the LTO, in which there are bulk structures in the middle of needle-like structures, along with some nanorod structures (which can be seen in Figures 1b, 1c, and 1d). This means the synthesis process failed

to fabricate LTO nanorods. The EDX mapping of the LTO, in Figure 2, shows that the titanium is distributed evenly.

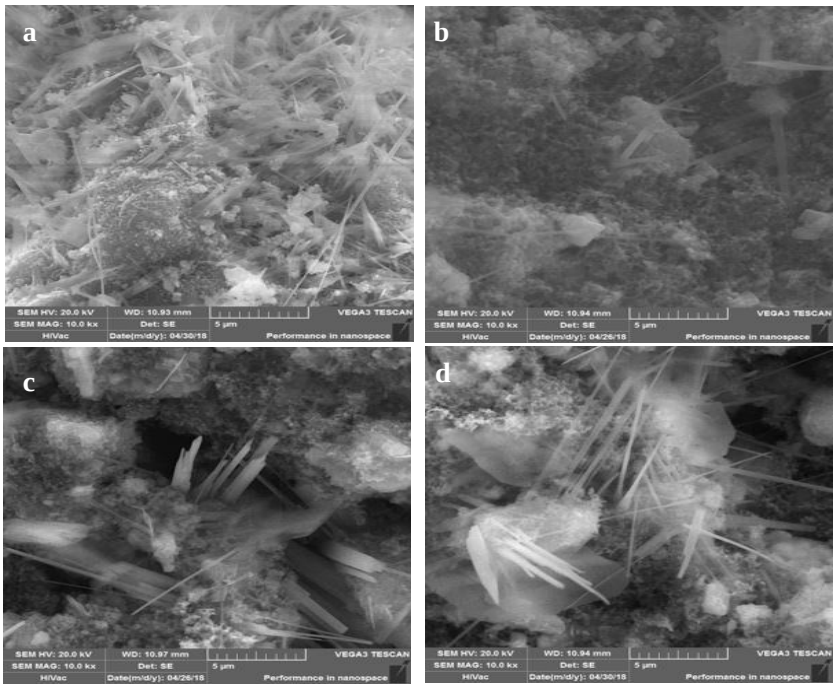

Figure 1 SEM images (mag. 10000×) of: (a) LTO; (b) LTO–AC/10% nano-Si; (c) LTO–AC/15% nano-Si; and (d) LTO–AC/20% nano-Si

However, there are impurities in the LTO, such as carbon, natrium, silicon, and chlorine. The hydrothermal process used NaOH as the precursor to make the nanorod template of TiO_2. After applying the hydrothermal method, the solution is washed by HCl. This process neutralizes the solution, giving it a pH of 7, but it also forms NaCl. Figure 2 shows the amount of natrium that is present, which is almost as much as the amount of titanium.

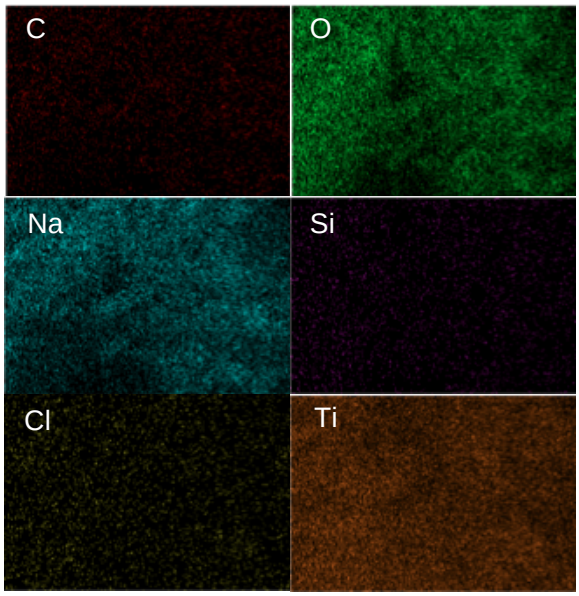

Figure 2 Image of SEM-EDX mapping of LTO

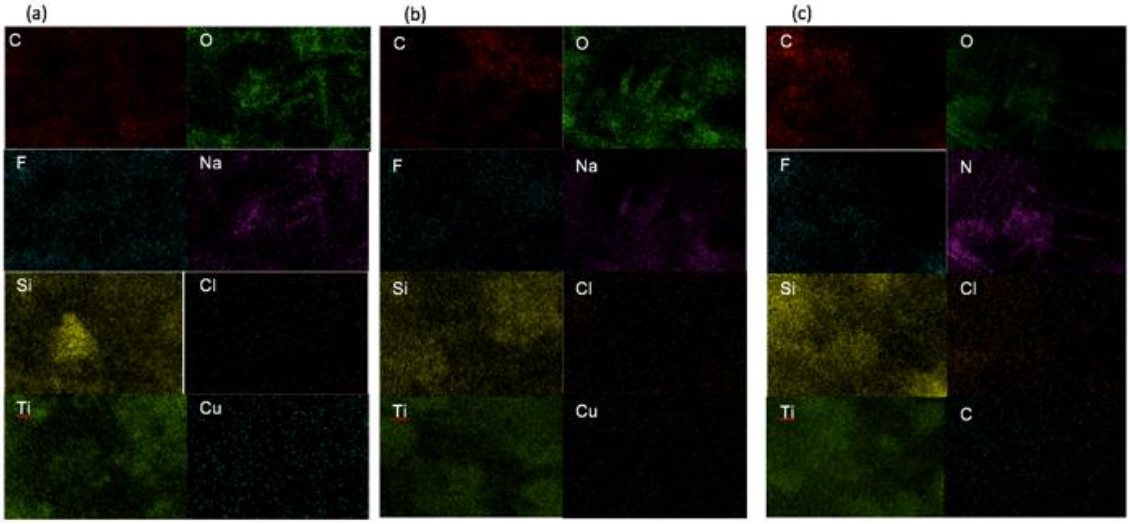

Figure 3 Images of the SEM-EDX mapping of: (a) LTO; (b) LTO–AC/10% nano-Si; (c) LTO–AC/15% nano-Si; (d) LTO–AC/20% nano-Si

The morphology of LTO–AC/10% nano-Si, LTO–AC/15% nano-Si, and LTO–AC/20% nano-Si are similar according to SEM images shown in Figures 3b, 3c, and 3d, respectively. The nanorod structures indicate the presence of LTO. There are two different contrasts in the agglomerated structures surrounding the nanorod structures: the dark contrast in the SEM images shows the material is not conductive, while the light contrast shows the material is conductive. As such, it can be concluded that the agglomerated structures in the dark contrast are nano-Si, while the agglomerated structures in the light contrast are AC. Agglomeration can reduce the surface area, leading to capacity loss, and it should therefore be avoided. Agglomeration happens during the slurry-making process. The agglomeration of the nano-Si can also be seen from the mapping images obtained from EDX (Figures 3a, 3b, and 3c). The nano-Si did not spread evenly and tended to be thick (i.e., agglomerated) in a certain region. The titanium also did not distribute equally. This is because, during the mixing process, the quantity of nano-Si powder is far more than the amount of LTO–AC powder. The grinding process on the agate mortar did not result in a good mixture of the nano-Si and LTO–AC powder. Each of the three samples also contained natrium and chlorine impurities, which resulted from the hydrothermal process during the synthesis of the LTO.

3.2. Analysis of LTO Composite by XRD

The synthesis process is supposed to form $Li_4Ti_5O_{12}$. Nonetheless, the structure that was formed was Li_2TiO_3, as shown in the results of the XRD test (Figure 4). This occurs because of the acid-washing after the hydrothermal process and the short single sintering time (Olszewska et al., 2017). Before the hydrothermal method was applied, the TiO_2 was mixed with an NaOH solution. The acid-washing (performed to neutralize the TiO_2) used a HCl solution and formed NaCl, and this could result in impurities in the sintering process.

3.3. Analysis of Surface Area by BET

The carbon was activated to make porous structures and increase the surface area, which helps to improve the conductivity of the battery (Bresser et al., 2012). A BET test was conducted to determine the surface area of the carbon and the LTO composites. The results are shown in Table 2. The AC had the largest surface area.

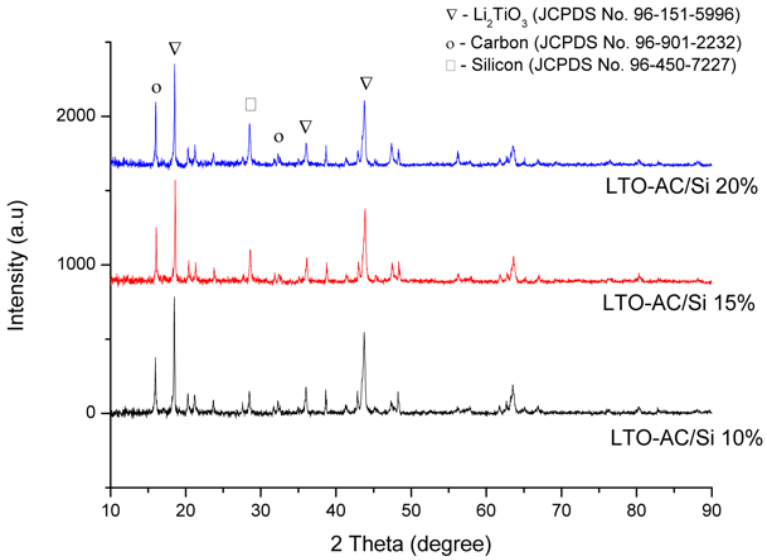

Figure 4 XRD graph of the LTO–AC/nano-Si composites

Table 2 Surface area based on BET test

Material	Surface Area (m^2g^{-1})
Activated Carbon (AC)	452.451
LTO–AC/10% nano-Si	63.075
LTO–AC/15% nano-Si	89.505
LTO–AC/20% nano-Si	133.943

The surface area of the composites indicated that AC does not affect the LTO composites; even though the AC had a surface area of >400 m^2g^{-1}, the largest surface area of the LTO composites was only 133 m^2g^{-1}. This is because the mixing method used to mix the AC, LTO, and nano-Si was only to grind them on an agate mortar. The surface area of the LTO composites with 10% nano-Si was smaller than that of the LTO composites with 15% and 20% nano-Si; this is because nano-Si provided a larger surface area, meaning there was a higher quantity of nano-sized particles in the LTO composites.

3.4. CV Analysis

The results of the CV tests of the LTO, LTO–AC/10% nano-Si, LTO–AC 15% nano-Si, and LTO–AC/20% nano-Si are shown in Figures 5a, 5b, 5c, and 5d, respectively. The XRD test showed that the most dominant phase that formed in all the samples was Li_2TiO_3, not $Li_4Ti_5O_{12}$. This result is parallel with the CV test result. The LTO peak (i.e., the peak of $Li_4Ti_5O_{12}$), which shows the working voltage of the samples, was not formed clearly in every sample. In Figure 5a, the LTO charge peak is at 1.655 V and 1.822 V, while the discharge peak is at 1.348 V and 0.528 V. The LTO peak in LTO–AC/10% nano-Si is at 1.656 V and 1.353 V; in LTO–AC/15% nano-Si is at 1.588 V and 1.359 V; and in LTO–AC/20% nano-Si is at 1.588 V and 1.359 V. The working voltage of the samples is relatively close to the theoretical working voltage of LTO, which is around 1.55 V. The peak also become less noticeable with the addition of nano-Si.

The CV results for all the LTO composites samples (AC–10% nano-Si, AC–15% nano-Si, and AC–20% nano-Si) do not show the silicon peaks. According to previous research, the silicon peak charge is at around 0.34 V (Ohtake, 2015). The absence of the silicon peaks indicates the formation of LixSi and amorphous silicon (Chen et al., 2015).

LTO–AC/15% nano-Si had the highest specific capacity, 140.7 mAh/g, while LTO–AC/20%

nano-Si had the lowest, 60.5 mAh/g. The specific capacity of LTO–AC/10% nano-Si was 128.4 mAh/g and of LTO was 139.9 mAh/g. These results show that the addition of nano-Si does not improve the specific capacity of the composite. LTO–AC/20% nano-Si had the lowest capacity because it contains a high quantity of nano-Si, which could pulverize, resulting in cracks on the composite.

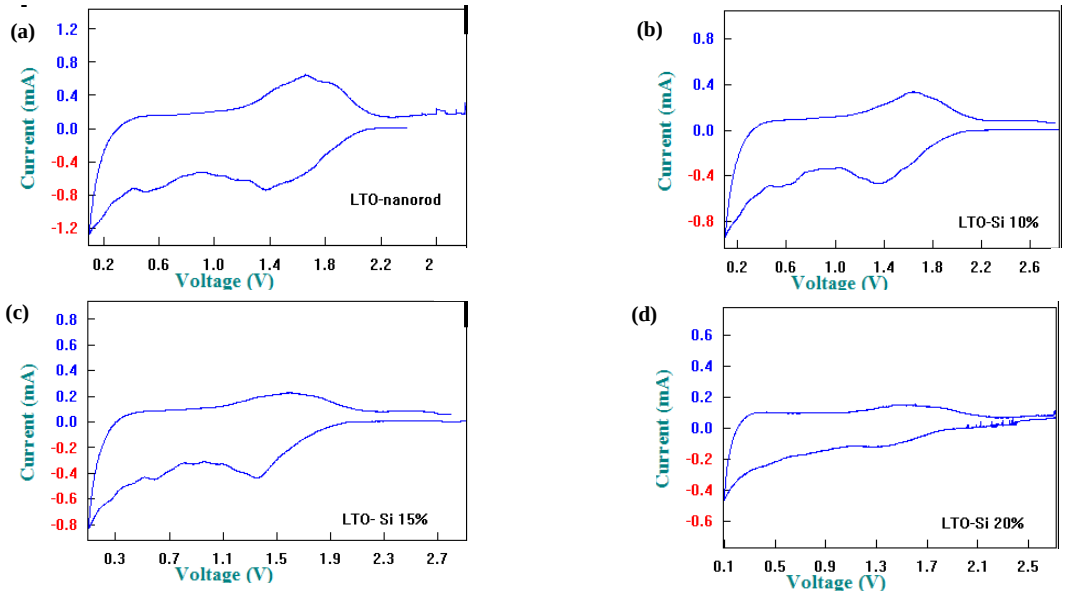

Figure 5 CV test graphs of: (a) LTO; (b) LTO–AC/10% nano-Si; (c) LTO–AC/15% nano-Si; and (d) LTO–AC/20% nano-Si

3.5. CD Analysis

A CD test was conducted to determine the performance of the battery. The test is done at several current rates, from 0.2 C to 20 C. 1 C means the CD current is given for 1 hour in order for the battery to reach its maximum capacity. The LTO and LTO–AC/15% nano-Si samples can perform up to 20 C, as can be seen in Figure 6a and 6c, respectively.

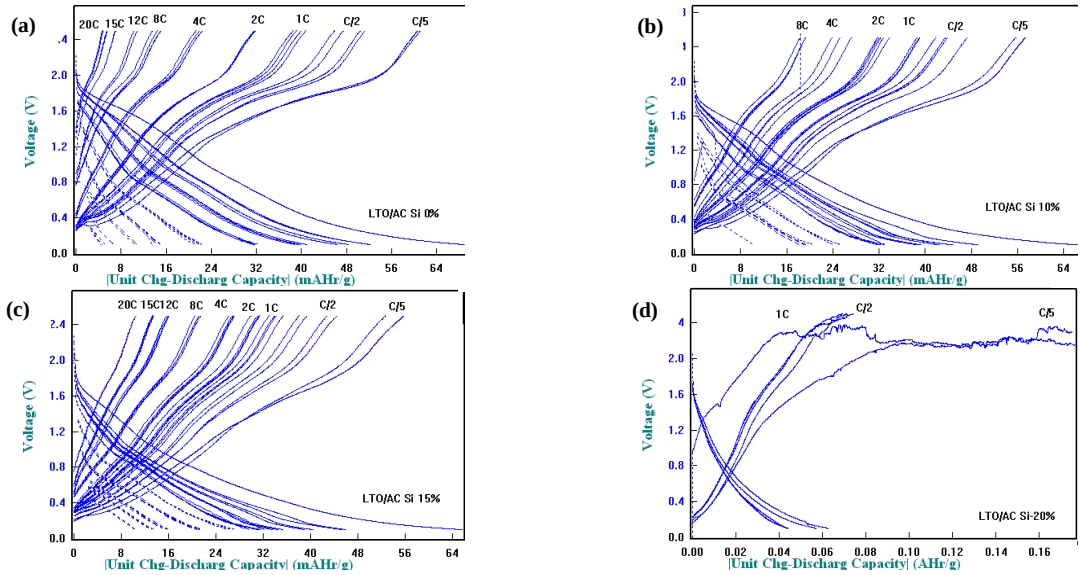

Figure 6 CD test graphs of: (a) LTO; (b) LTO–AC/10% nano-Si; (c) LTO–AC/15% nano-Si; and (d) LTO–AC/20% nano-Si

The LTO–AC/10% nano-Si sample can perform up to 8 C (Figure 6b) because of an insufficient amount of silicon in the composite. The LTO–AC/20% nano-Si sample is able to perform only up to 0.5 C (Figure 6d) because of the high percentage of silicon in the composite. The LTO is supposed to withstand the volume expansion of the silicon; however, if the quantity of the silicon is more than that of the LTO, the silicon will expand during cycling, causing a crack and disintegrating the electrode (Yoon et al., 2010). None of the graphs show a plateau, which is the characteristic of a CD graph of the battery, because Li_2TiO_3 is inactive as an electrode but can perform Li^+ transfer electrochemically (Chen et al., 2015).

The coulombic efficiency can be calculated using these CD tests. Coulombic efficiency is the ratio of discharge capacity to charge capacity. The equation is as follows:

$$\eta = \frac{C_{discharge}}{C_{charge}} \times 100\% \quad (1)$$

The coulombic efficiency of the LTO, LTO–AC/10% nano-Si, and LTO–AC/20% nano-Si samples (Figure 7) are close to 100%, with the lowest efficiency being 94.85%. This means that the samples have a good coulombic efficiency due to the zero-strain characteristic of the LTO (Lu et al., 2007).

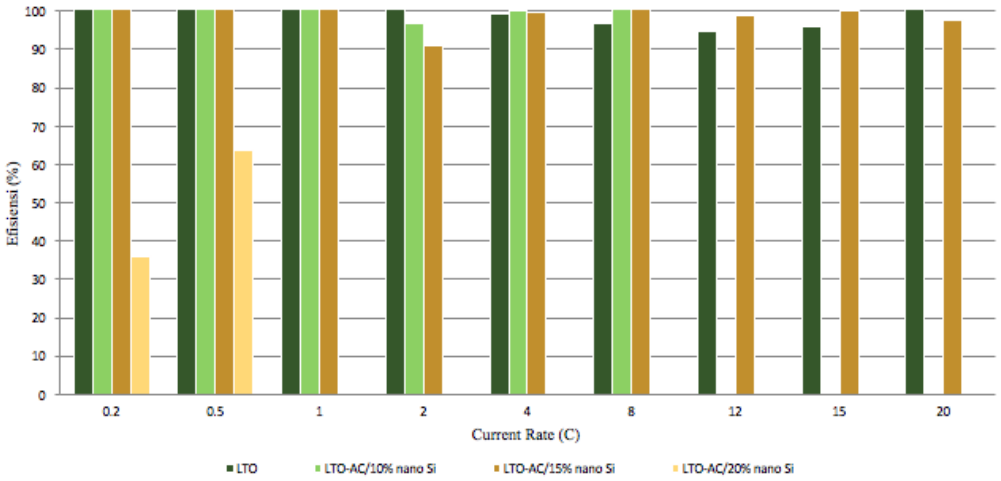

Figure 7 Graphs of Coulombic efficiency of LTO and LTO–AC/nano-Si composites

3.6. EIS Analysis

Resistance increases with the addition of nano-Si (Table 3). This is because silicon has low conductivity. Although AC was added to increase conductivity, based on the EIS test, the AC had no effect upon conductivity (Figure 8). This could be because the method used to mix the AC and the LTO was only grinding on an agate mortar before slurry making process.

Table 3 Rct number of LTO and LTO–AC/nano-Si composites based on EIS test eesult

Material	Surface Area (m^2g^{-1})
Activated Carbon (AC)	452.451
LTO–AC/10% Nano-Si	63.075
LTO–AC/15% Nano-Si	89.505
LTO–AC/20% Nano-Si	133.943

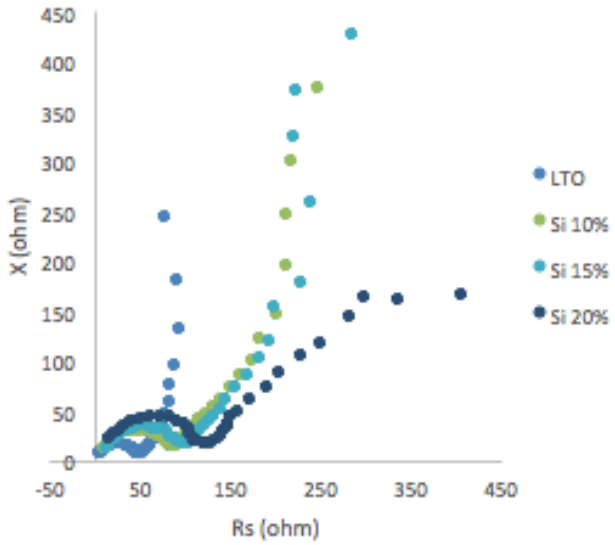

Figure 8 EIS graph of LTO–AC/nano-Si composites

4. CONCLUSION

The result of the synthesis process was the formation of nanorods and needle-like structures, proven by SEM, and the formation of the Li_2TiO_3 phase, proven by XRD. Agglomeration in the LTO–AC/nano-Si can be seen from the SEM and EIS results. The AC that was added did not affect the composite because the surface area of the composite was lower than the AC surface area, proven by BET; the electrical conductivity did not improve with the addition of AC, proven by EIS. Also, it was found that the higher the nano-Si percentage in the composite, the higher the charge transfer resistance and the lower the conductivity of the composite was. Further, the higher nano-Si percentage in the composite was, the higher the resistivity was found to be. The CV test results showed that LTO–AC/15% nano-Si had the highest specific capacity, at 140.7 mAh/h. It also showed that the LTO peak was not formed, because of the formation of Li_2TiO_3 phase. However, the potential of the peak is around 1.55 V, which is the theoretical potential of LTO. The CD test results showed that LTO and LTO–AC/15% nano-Si can perform up to 20 C, and both have a high coulombic efficiency.

5. ACKNOWLEDGEMENT

The authors would like to thank the Directorate Research and Public Services Universitas Indonesia for their financial support to do this research under HIBAH PITTA 2018 with contract No: 2377/UN2.R3.1/HKP.05.00/2018.

6. REFERENCES

Aurbach, D., Zinigrad E., Cohen, Y., Teller, H., 2002. A Short Review of Failure Mechanisms of Lithium Metal and Lithiated Graphite Anodes in Liquid Electrolyte Solutions. *Solid State Ionics*, Volume 148(3-4), pp. 405–416

Beaulieu, L.Y., Eberman, K.W., Turner, R.L., Krause, L.J., Dahn, J.R., 2001. Colossal Reversible Volume Changes in Lithium Alloys. *Electrochemical and Solid-State Letters*, Volume 4(9), pp. A137–A140

Bresser, D., Pailard, E., Copley, M., Bishop, P., Winter, M., Passerini, S., 2012. The Importance of "Going Nano" for High Power Battery Materials. *Journal of Power Sources*, Volume 219, pp. 217–222

Cai, R., Yu, X., Liu, X., Shao, Z., 2010. $Li_4Ti_5O_{12}$/Sn Composite Anodes for Lithium-ion Batteries: Synthesis and Electrochemical Performance. *Journal of Power Sources,* Volume 195(24), pp. 8244–8250

Cazetta, A.L., Vargas, A.M.M., Nogami, E.M., Kunita, M.H., Guilherme, M.R., Martins, A.C., Silva, T.L., Moraes, J.C.G., Almeida, V.C., 2011. NaOH-Activated Carbon of High Surface Area Produced from Coconut Shell: Kinetics and Equilibrium Studies from the Methylene Blue Adsorption. *Chemical Engineering Journal*, Volume 174(1), pp. 117–125

Chen, J., Zhao, H., He, J., Wang, J., 2011. Si/MgO Composite Anodes for Li-ion Batteries. *Rare Metals*, Volume 30(2), pp. 166–169

Chen, C., Agrawal, R., Wang, C., 2015. High Performance $Li_4Ti_5O_{12}$/Si Composite Anodes for Li-ion Batteries. *Nanomaterials (Basel)*, Volume 5(3), pp. 1469–1480

Gao, G., Liu, A., Hu, Z., Xu, Y., Liu, Y., 2011. Synthesis of $LiFePO_4$/C as Cathode Material by a Novel Optimized Hydrothermal Method. *Rare Metals*, Volume 30(5), pp. 433–440

Girishkumar, G., McCloskey, B., Luntz, A.C., Swanson, S., Wilcke, W., 2010. Lithium-air Battery: Promise and Challenges. *The Journal of Physical Chemistry Letters,* Volume 1(14), pp. 2193–2203

Kuo, Y.-C., Lin, J.-Y., 2014. One-pot Sol-gel Synthesis of $Li_4Ti_5O_{12}$/C Anode Materials for High-performance Li-ion Batteries. *Electrochimica Acta*, Volume 142, pp. 43–50

Li, T., Qiu, W., Zhang, G., Zhao, H., Liu, J., 2007. Synthesis and Electrochemical Characterization of 5 V $LiNi_{1/2}Mn_{3/2}O_4$ Cathode Materials by Low-Heating Solid-State Reaction. *Journal of Power Sources,* Volume 174(2), pp. 515-518

Li, T., Yang, J., Lu, S., 2012. Effect of Modified Elastomeric Binders on The Electrochemical Properties of Silicon Anodes for Lithium-ion Batteries. *International Journal of Minerals, Metallurgy, and Materials,* Volume 19(8), pp. 752–756

Li, Y., Pan, G.L., Liu, J.W., Gao, X.P., 2009. Preparation of $Li_4Ti_5O_{12}$ Nanorods as Anode Materials for Lithium-Ion Batteries. *Journal of the Electrochemical Society*, Volume 156, pp. A495–A499

Lu, W., Belharouak, I., Liu, J., Amine, K., 2007. Electrochemical and Thermal Investigation of $Li_{4/3}Ti_{5/3}O_4$ Spinel. *Journal of The Electrochemical Society,* Volume 154(2), pp. A114–A118

Maranchi, J.P., Hepp, A.F., Kumta, P.N., 2003. High Capacity, Reversible Silicon Thin-film Anodes for Lithiyoonum-ion Batteries. *Electrochemical and Solid-State Letters,* Volume 6(9), pp. A198–A201

Ohtake, T., 2015. Single Phase $Li_4Ti_5O_{12}$ Synthesis for Nanoparticles by Two Steps Sintering. *Scientific Research Publishing*, Volume 3(2), pp. 5–10

Olszewska, D., Rutkowska, A., Niewiedzial, J., 2017. Synthesis and Properties of Nickel-doped $Li_4Ti_5O_{12}$/C Nano-composite: An Anode for Lithium-ion Batteries. *Advances in Natural Sciences: Nanoscience and Nanotechnology*, Volume 8, pp. 1–6

Priyono, B., Syahrial, A.Z., Yuwono, A.H., Kartini, E., Marfelly, M., Rahmatullah, W.M.F., 2015. Synthesis of Lithium Titanate ($Li_4Ti_5O_{12}$) through Hydrothermal Process by Using Lithium Hydroxide (LiOH) and Titanium Dioxide (TiO2) Xerogel. *International Journal of Technology*, Volume 6(4), pp. 555–564

Stankulov, T., Obretenov, W., Banov, B., Momchilov, A., Trifonova, A., 2009. Silicon/Graphite Nano-structured Composites for a High-efficiency Lithium-ion Batteries Anode. *In*: Nanostructured Materials for Advanced Technological Applications, Reithmaier J.P., Petkov P., Kulisch W., Popov C. (eds.), Springer, Dordrecht, Netherlands, pp. 399–404

Syahrial, A.Z., Priyono, B., Yuwono, A.H., Kartini, E., Jodi, H., Johansyah, 2016. Synthesis of Lithium Titanate ($Li_4Ti_5O_{12}$) by Addition of Excess Lithium Carbonate (Li_2CO_3) in

Titanium Dioxide (TiO_2) Xerogel. *International Journal of Technology*, Volume 7(3), pp. 392–400

Wang, G.J., Gao, J., Fu, L.J., Zhao, N.H., Wu, Y.P., Takamura, T., 2007. Preparation and Characteristic of Carbon-coated $Li_4Ti_5O_{12}$ Anode Material. *Journal of Power Sources*, Volume 174(2), pp. 1109–1112

Yoon, K.R., Jung, J., Kim, I., 2010. Recent Progress in 1D Air Electrode Nanomaterials for Enhancing the Performance of Nonaqueous Lithium-oxygen Batteries. *ChemNanoMat: Chemistry of Nanomaterials for Energy, Biology, and More*, Volume 2(7), pp. 616–634

Zhao, B., Ran, R., Liu, M., Shao, Z., 2015. A Comprehensive Review of $L_{i4}Ti_5O_{12}$-Based Electrodes for Lithium-ion Batteries: The Latest Advancements and Future Perspectives. *Materials Science and Engineering*: *R: Reports*, Volume 98, pp. 1–71

Zhang, J., Wang, W., Xiao, J., Xu, W., Graff, G.L., Yang, G., Choi, D., Wang, D., Li, X., Liu, J., 2012. Silicon-based Anodes for Li-ion Batteries. *In*: Batteries for Sustainability, Brodd, R.J (ed.), Springer, New York, pp. 471–504

Zhou, Q., Liu, L., Tan, J., Yan, Z., Huang, Z., Wang, X., 2015. Synthesis of Lithium Titanate Nanorods as Anode Materials for Lithium and Sodium Ion Batteries with Superior Electrochemical Performance. *Journal of Power Sources*, Volume 283, pp. 243–250

Zhou, Y., Jiang, X., Chen, L., Yue, J., Xu, H., Yang, J., Qian, Y., 2014. Novel Mesoporous Silicon Nanorod as an Anode Material for Lithium Ion Batteries. *Electrochimica Acta*, Volume 127, pp. 252–258